Developmental Biology 395 (2014) 299–306

Contents lists available at ScienceDirect

Developmental Biology

journal homepage: www.elsevier.com/locate/developmentalbiology

Long-distance cell migration during larval development in the appendicularian, *Oikopleura dioica*

Kanae Kishi *, Takeshi A. Onuma, Hiroki Nishida

Department of Biological Sciences, Graduate School of Science, Osaka University, 1-1 Machikaneyama-cho, Toyonaka 560-0043, Osaka, Japan

ARTICLE INFO

Article history:
Received 18 July 2014
Received in revised form
30 August 2014
Accepted 7 September 2014
Available online 16 September 2014

Keywords:
Cell migration
Chordate
Appendicularian
Oikopleura dioica
Chemoattractant
Endodermal strand

ABSTRACT

The appendicularian, *Oikopleura dioica*, is a planktonic chordate. Its simple and transparent body, invariant cell lineages and short life cycle of 5 days make it a promising model organism for studies of chordate development. Here we describe the cell migration that occurs during development of the *O. dioica* larva. Using time-lapse imaging facilitated by florescent labeling of cells, three cell populations exhibiting long-distance migration were identified and characterized. These included (i) a multinucleated oral gland precursor that migrates anteriorly within the trunk region and eventually separates into the left and right sides, (ii) endodermal strand cells that are collectively retracted from the tail into the trunk in a tractor movement, and (iii) two subchordal cell precursors that individually migrate out from the trunk to the tip of the tail. The migration of subchordal cell precursors starts when all of the endodermal strand cells enter the trunk, and follows the same path but in a direction opposite to that of the latter. Labeling of these cells with a photoconvertible fluorescent protein, Kaede, demonstrated that the endodermal strand cells and subchordal cell precursors have distinct origins and eventual fates. Surgical removal of the trunk from the tail demonstrated that the endodermal strand cells do not require the trunk for migration, and that the subchordal cell precursors would be attracted by the distal part of the tail. This well-defined, invariant and traceable long-distance cell migration provides a unique experimental system for exploring the mechanisms of versatile cell migration in this simple organism with a chordate body plan.

Introduction

Migration of cells is an essential process for morphogenesis of the animal body and organ formation. Various cells in particular regions of embryos have specific fates and migrate individually or in groups until they reach their final destinations (Aman and Piotrowski, 2010). For example, primordial germ cells migrate as individual cells to the location of the gonad during embryogenesis of the mouse, zebrafish, fly and other animals (Richardson and Lehmann, 2010). Another mode of cell migration is collective migration. The sensory lateral line primordium of the zebrafish migrates posteriorly as a group of cells depositing neuromasts during larval development (Ghysen and Dambly-Chaudière, 2004). Neural crest cells in vertebrates delaminate from the neural tube and migrate collectively as cellular streams to all regions of the body (Knecht and Bronner-Fraser, 2002). While these examples highlight the diversity of cell migration, it remains largely unclear how versatile movements of different types of cells are orchestrated for formation of the functional body.

The appendicularian, *Oikopleura dioica,* is a pelagic or planktonic tunicate that retains a swimming tadpole shape during its entire life. For several reasons, it possesses certain advantages as a model animal (Nishida, 2008): (1) It possesses the basic body plan of chordates; (2) its development is rapid, and organogenesis is completed within 10 h post-fertilization (hpf) to form a functional body; (3) it has a small number of cells; for example, there are only 550 cells at hatching (Stach et al., 2008); (4) the body is transparent throughout life. These features make *O. dioica* a useful species for comprehensive studies of chordate development. Furthermore, we have recently established techniques for introducing fluorescent protein mRNAs into embryos for imaging and a RNAi method for gene knockdown (Omotezako et al., 2013).

Morphogenesis and cell lineages during embryogenesis of *O. dioica* have been well described (Delsman, 1910; Fujii et al., 2008; Stach et al., 2008), as is the case for ascidians (Conklin, 1905; Nishida, 1987). These studies have shown that the cleavage pattern and cell lineages of *O. dioica* are invariant and determinative. In contrast, much less is known about larval development after hatching (Nishida, 2008). Descriptions of larval morphogenesis have been restricted to those based on observations using conventional microscopy (Delsman, 1910, 1912; Fenaux, 1998; Nishida, 2008). In a series of notable studies, Delsman (1910, 1912) carried

* Corresponding author. Fax: +81 6 6850 5472.
E-mail address: kkishi@bio.sci.osaka-u.ac.jp (K. Kishi).

http://dx.doi.org/10.1016/j.ydbio.2014.09.006
0012-1606/

out detailed observations of *O. dioica* at various embryonic and larval stages collected directly from the ocean with a plankton net. On the basis of his investigations, he suggested that some larval cells migrate extensively; oral gland precursor cells migrate anteriorly and give rise to left and right oral glands, and the endodermal strand cells in the tail migrate into the trunk and then two cells of them come back into the tail to be subchordal cells after hatching stage (Delsman, 1910, 1912).

In the present study, we monitored the larval development of *O. dioica* using time-lapse microscopic imaging, florescent cell labeling, and confocal microscopy. We found three cell populations that exhibit long-distance migration: (i) Oral gland precursor that migrates anteriorly within the trunk region; (ii) endodermal strand cells in the tail that are absorbed into the trunk; and (iii) two subchordal cell precursors that migrate along the same path as endodermal strand cells, but in an opposite direction, in the tail. Our results basically support Delsman's observations, with two exceptions: the oral gland precursor migrates as a single syncytium, and endodermal strand cells and subchordal cells each originate from distinct embryonic regions. Microsurgical separation of the trunk and tail revealed that migration of endodermal strand cells does not require the trunk, whereas migration of subchordal cell precursors requires the distal half of the tail.

Materials and methods

Laboratory culture of O. dioica

Live wild animals were collected at Sakoshi Bay and Tossaki Port in Hyogo, Japan, and sorted and cultured over generations in the laboratory, as described previously (Bouquet et al., 2009; Nishida, 2008; Omotezako et al., 2013). It has a shot life cycle (5 days at 20 °C). In brief, they were reared in 10-l containers using two types of artificial seawater, REI-SEA Marine (IWAKI, Tokyo, Japan) or MARINE ART BR (Tomita Pharmaceutical, Tokushima, Japan) with stirring (15 rpm) at 20 °C and were fed the algae *Isochrysis galbana* and *Rhinomonas reticulata*, the diatom *Chaetoceros calcitrans*, and the cyanobacterium *Synechococcus* sp. The animals become sexually mature and spawn within 5 days after fertilization.

Injection of the ovary with mRNAs

H2B-EGFP or H2B-mCherry and PH-YFP mRNAs were used to visualize the nucleus and cell membrane, respectively. *H2B-EGFP* and *H2B-mCherry* cDNAs were subcloned into the pSD64TF vector (a gift from Dr. T. Snutch, University of British Columbia, Canada), which includes the SP6 polymerase promoter and the 5′- and 3′-UTR sequences of the β-globin mRNA of *Xenopus laevis*, as described previously (Omotezako et al., 2013). PH-YFP cDNA was a gift from Dr. A. Gregorio (Weill Medical College of Cornell University, NY). It was inserted into the HTB(N) vector that carries *Halocynthia roretzi* tubulin UTRs. To generate pSD64TF-nls-Kaede (Kaede with a nuclear localization signal), the *H2B-mCherry* sequence of pSD64TF-H2B-mCherry was replaced by *nls-Kaede* cDNA (a gift from Dr. K. M. Kwan, University of Utah). These plasmids were linearized with *Xba* I or *Pst* I and used as templates for in vitro transcription. Capped mRNAs were synthesized with a mMESSAGE mMACHINE kit (Ambion, Austin, TX) and Poly (A) was added with a Poly (A) Tailing kit (Ambion).

For live fluorescence imaging of embryos, synthetic mRNAs were injected into the ovary of a Day 5 animal as described previously (Omotezako et al., 2013). Because growing oocytes are connected to shared cytoplasm through a pore called the ring canal within the ovary (Ganot et al., 2007), injected mRNAs spread through the gonad with a gradient and were eventually incorporated into full-grown oocytes. 1–3 μg/μl mRNA solution containing 1 mg/ml phenol red was injected. The spawned eggs were fertilized and cultured at 20 °C. Embryos with fluorescence were selected before hatching and used for time-lapse video recording.

Microscopy and time-lapse analysis

Nomarski microscopy images were captured using an Olympus BX61 microscope with UPlanSApo 40 × /0.90 or LUMPlanApo 40 × /0.80 Water (non-cover water lens) or UPlanApo 100 × /1.35 Oil Iris, and the Lumina vision software package (Mitani Corporation, Tokyo, Japan). Fluorescence time-lapse movies were acquired using DeltaVision (Corns Technology, Tokyo, Japan) with U-Plan S-Apo 20 × /0.75 or U-Apo 40 × /1.35 Oil (Olympus). Some 3D images were acquired using a Zeiss LSM710 confocal microscope with Plan-Apo 40 × /0.95 Korr and the ZEN software package.

To immobilize swimming hatched larvae for time-lapse video recording, three different mounting methods were employed. First, the tail was cut off or crushed with a fine knife made from Tungsten. Second, larvae were embedded in 0.5% Low Melting Point Agarose XP (Nippon Gene, Tokyo, Japan) dissolved in artificial seawater. For this, larvae were placed gently onto a glass bottom dish and then 200 μl of the agarose solution was poured over them. Third, larvae were placed on glass slides and gently pressed with a coverslip in 0.25% Agarose XP. Images and movies were analyzed using ImageJ (NIH).

Cell tracing using the photoconvertible protein, Kaede

nls-Kade mRNA was injected into the embryos, and hatched larvae showing green fluorescence were used. To convert the green fluorescence to red, larvae were exposed to ultraviolet light (UV) for 1 s under an Olympus BX-61 microscope. The field diaphragm was adjusted so that only to the tail or trunk region was exposed to UV light. The distribution of labeled cells was analyzed 6 h after photoconversion.

Microdissection experiment

To analyze the mechanisms responsible for cell migration, the trunk or tail was amputated using the tungsten knife at various time points. The animals were anesthetized with 0.015% MS222 (Sigma, St. Louis, MO) in seawater. The dissected tails or trunks were mounted into 0.25% agarose XP on micro glass slides, and time-lapse video recording was carried out by Nomarski microscopy.

SYTOX Green nuclear staining

Adult animals were fixed in 4% PFA/0.1 M MOPS/0.5 M NaCl/0.2% TritonX-100/5 mM EGTA at 4 °C overnight. After washing 3 times (10 min per wash at RT) in Solution A (0.5 M NaCl/10 mM Tris HCl (pH 8.0)/50 mM EDTA/0.1% Tween), samples were treated with 100 μg/ml RNaseA in solution A at 37 °C for 2 h. The samples were then washed once in Solution A for 5 min, and 3 times in TN buffer (50 mM Tris–HCl (pH 7.4)/0.15 mM NaCl) for 10 min each time, and finally stained with 5 μM S7020 SYTOX Green (Invitrogen, Tokyo, Japan) in TN buffer at 4 °C overnight. After washing with TN buffer, the specimens were mounted in VECTASHIELD (Funakoshi, Tokyo, Japan).

Results

O. dioica embryos hatch at 3 h after fertilization at 20 °C, and then larval development continues for 7 h for completion of organogenesis and formation of a fully functional body with similar organization to that of adults. The hatched larvae are 200 μm long. In this study, we employed Normaski (DIC) microscopy, fluorescence cell labeling and confocal microscopy to characterize the larval development of *O. dioica*. Our time-lapse video recordings revealed three cell populations that show long-distance migration: the oral gland precursor, endodermal strand cells, and subchordal cell precursors.

Oral gland precursor migrates as a syncytium containing four nuclei

To observe larval development, we cut off the tail to prevent motility. Even if the larva lacks the tail, the trunk develops normally for several hours, except that they eventually lack a rectum for the reason mentioned later.

In the trunk of hatched larvae, a conspicuous migrating cell was observed (Fig. 1A, Movie S1). It migrated anteriorly after emergence in the posterior region of the trunk at 1.5–4.0 h post-hatching (hph). On the basis of the final destination, shape and number, this migrating cell is the precursor cell of the "oral gland", corresponding to Delsman's description. The oral gland is a pair of large cells in the vicinity of the mouth present between the endostyle and epidermis in adults (Fig. 1B). In Appendicularia, the oral gland is present only in the genera *Oikopleura, Stegosoma,* and *Folia*, which also have subchordal cells in the tail, but its function is still controversial (Fredriksson and Olsson, 1991).

Supplementary material related to this article can be found online at http://dx.doi.org/10.1016/j.ydbio.2014.09.006.

Each oral gland cell in adults had two nuclei when visualized by SYTOX Green nuclear staining (Fig. 1C). Troedsson et al. (2007) also reported that oral gland cell contains two nuclei. H2B-EGFP mRNA was introduced into larvae to visualize and trace the movement of the nuclei of the oral gland precursor. As shown in Fig. 1D and E, the oral gland precursor had four nuclei when it started anterior migration at 1.5–2 hph. The oral gland precursor elongated during

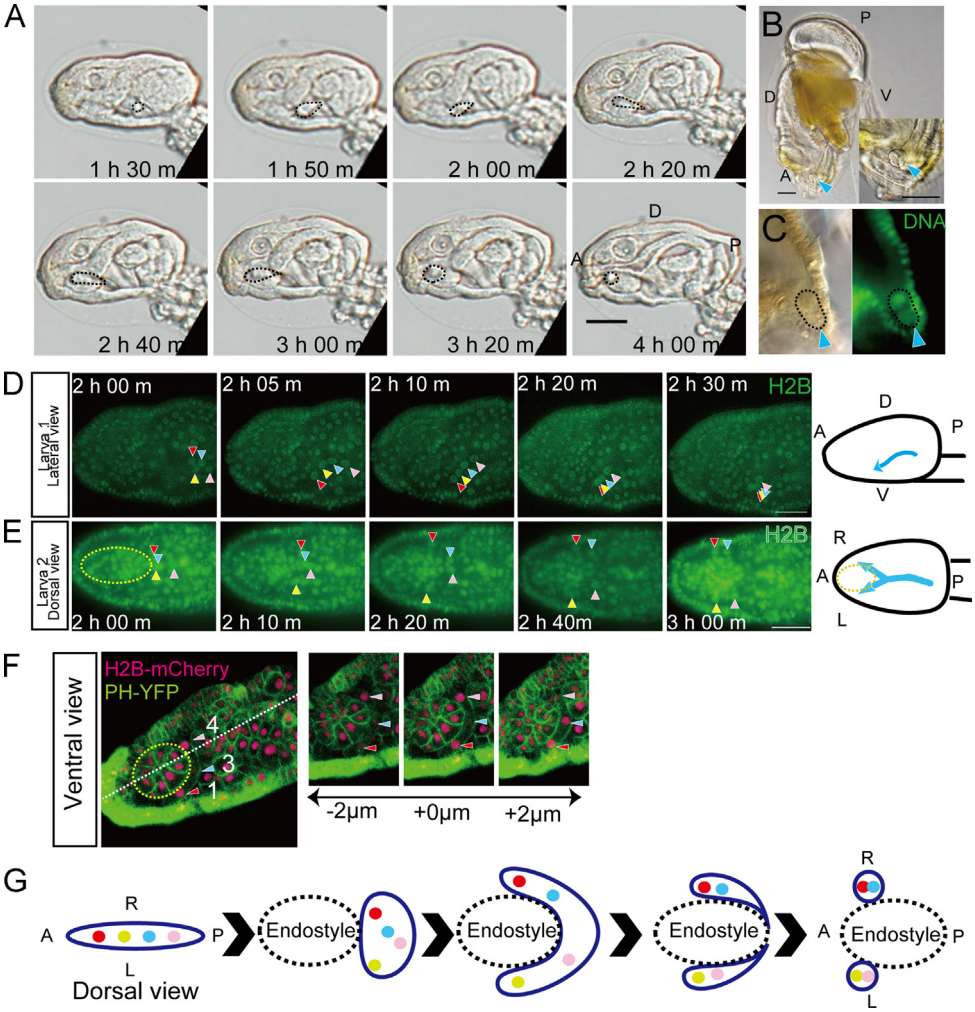

Fig. 1. Migration of oral gland precursors. (A) Images from a time-lapse movie taken using Nomarski optics (Movie S1). The tail was amputated just after hatching to prevent swimming. The oral gland precursor (outlined by dashed line) migrates anteriorly within the trunk. ((B) and (C)) Oral gland in the adult animal. (B) Nomarski image of the trunk. (C) DNA was stained by SYTOX Green. Oral gland is outlined by a dashed line. Two large nuclei are observed in an oral gland cell. ((D) and (E)) Images from a fluorescence time-lapse movie (Movie S2). Four nuclei (Red, yellow, cyan, pink arrowheads indicate the first, second, third and fourth nuclei, respectively.) migrate anteriorly in a line ((D) lateral view), two going to the left side of the endostyle (yellow circle) and the other two to the right ((E) dorsal view). Schematic diagrams are shown on the right. Times are elapsed time after hatching. (F) Slices from a 3D image taken by confocal microscopy at 2.5 hph. Ventral view. Green, membrane (PH-YFP); red, nuclei (H2B-mCherry); white line, median line; yellow circle, endostyle; numbers represent order of nuclei from the anterior. The second nucleus is out of focus, but it is located in a left-anterior position. (G) Schematic diagrams showing migration of the oral gland precursor. Dorsal view. Blue solid line outlines the oral gland precursor. Broken represents the endostyle. D, dorsal; V, ventral; A, anterior; P, posterior; L, left; R, right. Scale bar, 50 μm.

migration, the four nuclei being aligned as a single line (Fig. 1D and G, Movie. S2). It then became U-shaped when it reached the midline endostyle that settles on the migratory pathway, and was eventually pulled apart at the bottom of U-shaped cell into left and right cells that each inherited two nuclei at 3 hph (Fig. 1E and G, Movie. S2 and S3). The anterior portion of the migrating oral gland precursor had lamellipodium-like protrusions (Movie S3). The four nuclei showed an invariant pattern of partitioning during division of the oral gland precursor. The first and third nuclei in the row went to the left, while the second and fourth went to the right ($n=6/6$) (Movie S2).

Supplementary material related to this article can be found online at http://dx.doi.org/10.1016/j.ydbio.2014.09.006.

We then examined whether the oral gland precursor is a syncytium or a cell mass. Embryos were double-labeled with fluorescent markers for the nucleus (H2B-mCherry) and cell membrane (PH-YFP) and observed by confocal microscopy. As shown in Fig. 1F, no cell membrane was present between the four nuclei, demonstrating that the oral gland precursor migrates as a syncytium with four nuclei and then divides into two cells, each containing two nuclei (Fig. 1G). It is likely that these cells each continue to have two nuclei until the end of life (Fig. 1C).

Endodermal strand cells and subchordal cell precursors migrate along the same path but in opposite directions

The tail undergoes 90° counterclockwise rotation relative to the trunk during embryogenesis (Delsman, 1910; Stach et al., 2008; Nishida, 2008). As a result, the dorsal-ventral axis and left-right axis of the tail shifts by 90° when compared with those in ascidians and, the neural tube is on the left side of the tail and the endodermal strand is on the right side. Subchordal cells are present in the adult tail of some appendicularian genera. In *O. dioca*, two subchordal cells are located on the right side of the notochord in adults (Fig. 2A) (Fredriksson and Olsson, 1991), and have many protrusions. Their physiological functions remain elusive and their developmental origin has not been described.

The endodermal strand cells and subchordal cells showed long-distance migration between the trunk and tail regions (Fig. 2, Movie S4). The endodermal strand is the strand of 16 cells that lie in a single line (Stach et al., 2008). Using PH-YFP labeling, we confirmed that each nucleus was separated by a plasma membrane. As shown in Fig. 2B, the cells migrated collectively from the tail to the trunk at 0.75 hph to 2 hph. Time-lapse video recording showed that the migration velocity of the endodermal strand cells remained constant until their arrival at the trunk (Movie S4). Immediately after the entire endodermal strand had been absorbed into the trunk, two subchordal cell precursors in the trunk started posterior migration into the tail at 2 hph to 3 hph (Fig. 2B and C). These two cells migrated while maintaining a constant distance between them, and finally stopped moving in the posterior part of the tail, still with a space between them, as their final destination and remained there until the adult stage. Labeling of larval nuclei with H2B-EGFP also showed that the endodermal strand and subchordal cells are populations of mononuclear cells (Fig. 2C, Movie S4).

Supplementary material related to this article can be found online at http://dx.doi.org/10.1016/j.ydbio.2014.09.006.

The subchordal cell precursors migrate along the right side of the notochord in the space that has been filled with endodermal strand cells (Fig. 2B, Movie S4). Therefore, the endodermal strand and subchordal cell precursors share the same migratory route, although they migrate in opposite directions. High-magnification images showed that, during migration, subchordal cells had lamellipodium-like protrusions that were more frequent on the anterior edge (Fig. 2D, Movie S5). On the other hand, the endodermal strand cells did not show such activity during their migration (see Movie S7).

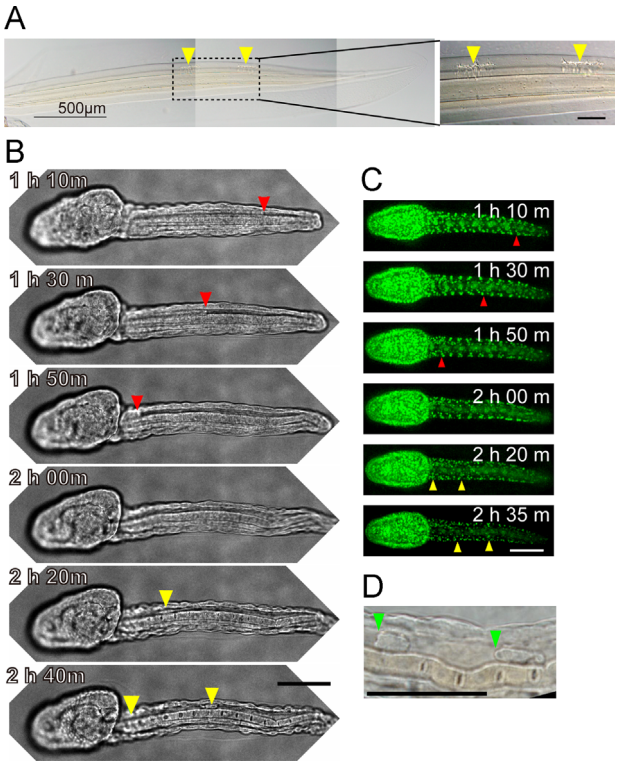

Fig. 2. Migration of endodermal strand cells and subchordal cell precursors. (A) Subchordal cells in the tail of an adult animal. Two subchordal cells (yellow arrowheads) lie on the right side of the notochord. (B) Images from a time-lapse movie taken with Nomarski optics. The larva was embedded in low-melting-point agar. Dorsal view. Endodermal strand of the tail is absorbed into the trunk. Red arrowheads indicate the posterior end of the endodermal strand, and yellow arrowheads indicate the subchordal cell precursors. (B) Images from a fluorescence live imaging movie (Movie S4). Ventral view. Green, nuclei (H2B-EGFP). (C) High-magnification image of subchordal cell precursors taken using Nomarski optics (Movie S5). Green arrowheads indicate the lamellipodia. Scale bars, 50 μm.

Supplementary material related to this article can be found online at http://dx.doi.org/10.1016/j.ydbio.2014.09.006.

Supplementary material related to this article can be found online at http://dx.doi.org/10.1016/j.ydbio.2014.09.006.

The fate of endodermal strand cells and the origin of subchordal cell precursors

We examined the eventual fates of the endodermal strand cells and the origin of subchordal cell precursors. For this purpose, nls-Kaede mRNA was introduced into *O. dioica* larvae. Kaede is a photoconvertible green fluorescent protein whose fluorescence is irreversibly converted to red by exposure to UV (Ando et al., 2002). Nls-Kaede is a modified version of Kaede containing a nuclear localization signal at its N-terminus (Kwan et al., 2012). As shown in Fig. 3A, the green fluorescence was observed in nuclei of every cell in the developing larva. Upon UV irradiation (white circle), this signal was converted to red in the illuminated region (Fig. 3A and C).

To trace the endodermal strand cells, the larval tail was labeled with red fluorescence prior to the start of cell migration (Fig. 3A). The distribution of labeled cells was then examined at 6 hph, when larvae had almost completed organ formation. In the trunk, most of the rectum was labeled with red fluorescence (Fig. 3B, $n=7/7$). In addition, we observed a small number of red cells in

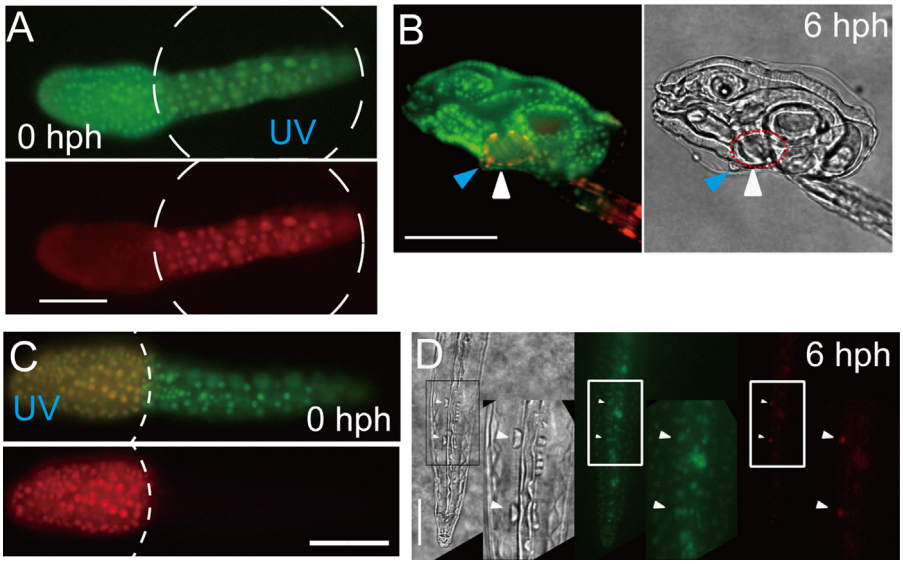

Fig. 3. The fate of endodermal strand cells and the origin of subchordal cell precursors. ((A) and (C)) Larvae express nls-Kaede. The region of UV illumination is outlined by dashed circles. The fluorescence only in the tail (A), or only in the trunk (C), turned red at 0 hph. ((B) and (D)) Larvae observed at 6 hph. (B) Six hours after UV illumination of the tail. The rectum (white arrowheads and red circle) shows red fluorescence. Blue arrowheads indicate position of the anus. (D) Six hours after UV illumination of the trunk. In the tail, subchordal cell precursors (white arrowheads) show red fluorescence. Scale bar, 50 μm.

the intestine and right stomach of some specimens. These observations clearly indicated that the endodermal strand cells give rise to the posterior part of the digestive tract.

Another issue is whether the subchordal cell precursors originate from the trunk or from the tail. A closer view of the base of the tail and trunk region (Movie S6) showed that the subchordal cell precursors appeared to have a distinct origin, and were not derived from the retracted endodermal strand cells. To confirm this, the larval trunk was labeled with red fluorescence immediately after hatching (Fig. 3C). If the subchordal cell precursors are derived from the trunk, then red florescence would be detected in the subchordal cells after migration. Indeed, red fluorescence was detected in the subchordal cells of larvae at 6 hph (Fig.3D). No other cells in the tail were labeled. Therefore, the subchordal cells were derived from the trunk, and not from retracted endodermal strand cells, and the endodermal strand and subchordal cell precursors have distinct and separate origins in hatched larvae.

Supplementary material related to this article can be found online at http://dx.doi.org/10.1016/j.ydbio.2014.09.006.

Migration of endodermal strand cells does not require the trunk and the posterior region of the tail

The migration of endodermal strand cells and subchordal cell precursors is uni-directional and stereotyped in the tail. In many cases of cell migration, diffusible signaling molecules work as chemoattractants or repellents (David et al., 2002; Raz, 2004; Lecaudey et al., 2008). The directional cell migration found in the present study would be also mediated by attractants or repellents emanating from the trunk or tip of the tail. To test this possibility, surgical amputation was carried out to remove these tissues, and the larvae treated in this way were monitored for cell migration using time-lapse video recording (Figs. 4 and 5).

To investigate whether the trunk is required for migration of endodermal strand cells, the trunk was amputated at 0 hph. However, the endodermal strand cells migrated normally, went out from the anterior cut edge, and became stuck outside the tail (Fig. 4A). Thus it is likely that the endodermal strand cells do not require the trunk for initiation of migration. To test whether the anterior-most endodermal strand cells function as 'leading cells' to guide or pull posterior cells, we amputated the trunk at 1.5 hph when the anterior half of the endodermal strand cells had entered the trunk (Fig. 4B, Movie S7). The remaining posterior endodermal strand cells still migrated to outside the tail. Likewise, migration of the endodermal strand cells occurred even after additional amputation of the distal half of the tail (Fig. 4C). Thus, it is unlikely that the trunk or posterior tail at this stage of amputation is required for the migration of endodermal strand cells.

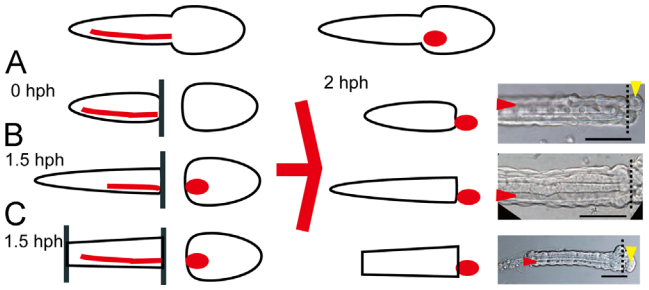

Fig. 4. Migration of endodermal strand cells does not require the trunk and the posterior region of the tail. ((A)–(C)) Microdissection experiments for the endodermal strand. (Top) Normal larvae. Red cells are those of the endodermal strand. (A) The trunk was removed from the tail at 0 hph. The endodermal strand migrated anteriorly and exited from the tail ($n=26/26$). (B) The trunk was removed at 1.5 hph when the anterior half of the endodermal strand cells has already been absorbed into the trunk. The endodermal strand migrated anteriorly ($n=10/10$). One example is shown in Movie S7. (C) The trunk and the distal half of the tail were removed at 1.5 hph. The endodermal strand migrated anteriorly ($n=6/6$). Photos on the right were taken at 2 hph. Notochord is present in the center of the tail. Red arrowheads, right side of the tail where the endodermal strand was located. Yellow arrowheads, endodermal strand cells that exited the tail. Scale bar, 50 μm.

Supplementary material related to this article can be found online at http://dx.doi.org/10.1016/j.ydbio.2014.09.006.

Delsman (1910, 1912) proposed that the oral gland precursor migrated as a sausage-shaped cell-rope and originated from the absorbed endodermal strand cells. If so, amputation of the tail including the endodermal strand would lead to absence of the oral gland cell. However, the oral gland precursor migrated normally in the trunk of larvae whose tail had been removed at 0 hph (Fig. 1A), although they failed to develop a rectum, which is derived from

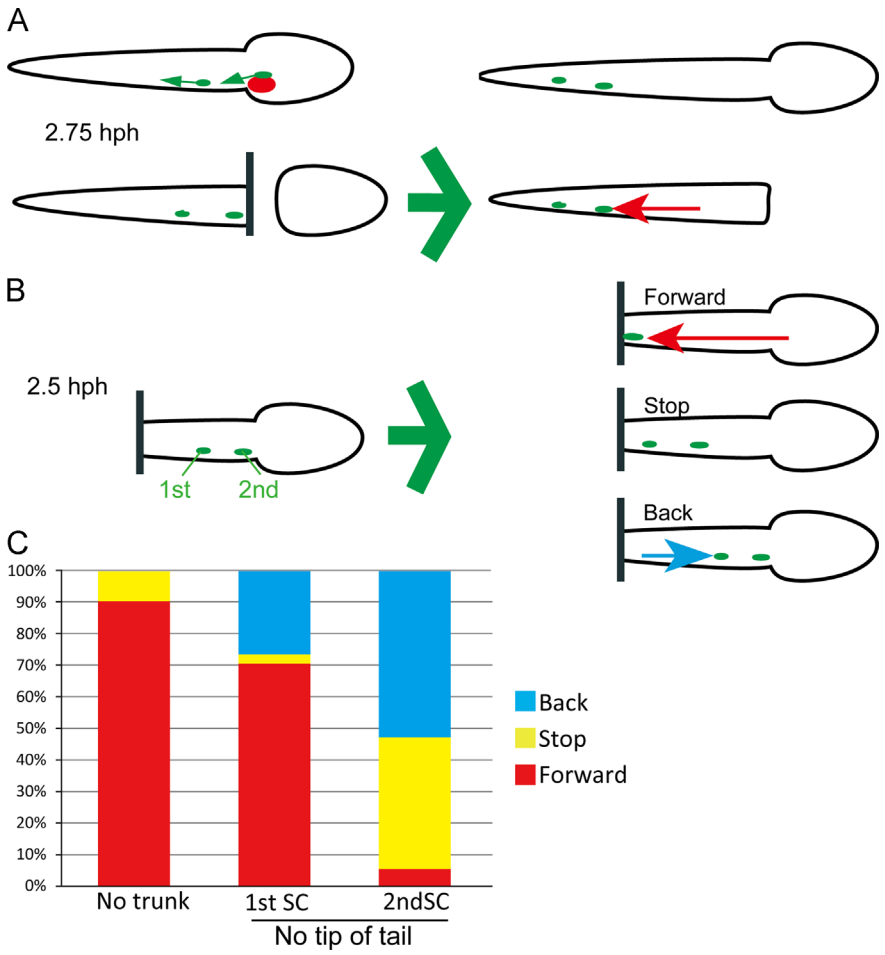

Fig. 5. Mechanisms of migration of subchordal cell precursors. ((A) and (B)) Microdissection experiments for subchordal cell precursors. (A) The trunk was removed at 2.5 hph just after two subchordal cell precursors had entered the tail, and the precursors migrated posteriorly, as in a normal larva ($n=9/10$). (B) The distal half of the tail was removed at 2.5 hph. Three kinds of migration were observed as a result: "Forward" means that the precursors migrated posteriorly, as in a normal larva. "Stop" means that the precursors stopped before they reached the cut end. "Back" means that the precursors migrated anteriorly. (C) Frequencies of each phenotype.

the endodermal strand cells. Therefore, the oral gland cells do not originate from the endodermal strand cells.

Posterior portion of the tail is required for proper migration of subchordal cell precursors

Next, we monitored the migration of subchordal cell precursors in larvae subjected to amputation (Fig. 5). First, the trunk was amputated at 2.5 hph, just after two subchordal cell precursors had entered the tail (Fig. 5A). The two subchordal cell precursors migrated normally ($n=9/10$), as observed in unamputated controls, suggesting that the migration is not dependent on repulsion from the trunk. In contrast, amputation of the posterior portion of the tail perturbed the movement of the subchordal cell precursors (Fig. 5B and C). The resulting phenotypes were categorized into three groups based on their cell behavior: "Forward", "Stop" and "Back" (Fig. 5B, Movie S8). In the Stop phenotype, the subchordal cell precursors migrated posteriorly at the initial stage but then stopped their migration and did not arrive to the cut end of the tail (Fig. 5B, middle panel). In the Back phenotype, the precursors migrated in an anterior direction toward the trunk (Fig. 5B, lower panel). The ratios of these phenotypes differed between the first and second subchordal cell precursors (Fig. 5C): for the first precursor 2.9% ($n=1/34$) and 26.5% ($n=9/34$) showed the Stop and Back phenotypes, whereas for second precursor 41.2% ($n=14/34$) and 52.9% ($n=18/34$) did so, respectively (Fig. 5C). These types of abnormal behavior were rarely observed in larvae whose trunk had been amputated. These results indicate that the posterior portion of the tail is required for posterior migration of subchordal cell precursors.

Supplementary material related to this article can be found online at http://dx.doi.org/10.1016/j.ydbio.2014.09.006.

Discussion

We studied the larval development of *O. dioica*, and showed that there are at least three sets of cells showing long-distance migration: the oral gland precursor, endodermal strand cells, and subchordal cell precursors. The oral gland precursor migrates anteriorly in the trunk as a syncytium with four nuclei and separates into two cells, each possessing two nuclei. Endodermal strand cells are absorbed from the tail into the trunk as a cell strand. Subchordal cell precursors migrate from the trunk to the tail as two individual cells along the same path but in a direction opposite to that of the endodermal strand cells (Fig. 6A). We thus confirmed the descriptions of Delsman (1910, 1912), who first described the migration of these cells on the basis of microscopic observations of fixed and live embryos and larvae. Nonetheless, the imaging techniques used in the present study revealed several differences from his descriptions. For instance, Delsman suggested that the endodermal strand is withdrawn into the trunk and that two endodermal strand cells come back into the tail as subchordal cells (Delsman, 1910, 1912). However, our time-lapse video

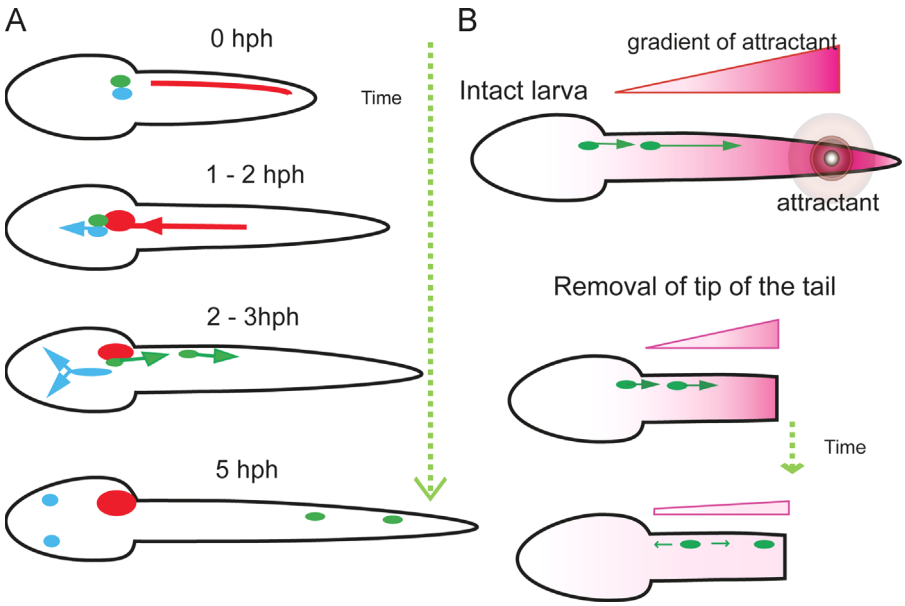

Fig. 6. Schematic diagrams of migration. (A) Schematic representations of the three types of migration at four stages. Dorsal view. Red, endodermal strand; green, subchordal cell precursors; blue, oral gland precursors. (B) Model for subchordal cell migration, in which there are diffusible chemoattractants extending from the distal half of the tail. In the intact larva, attractants diffuse from the source and form a concentration gradient in the tail. Subchordal cell precursors sense this gradient and migrate posteriorly, toward the source. When the source is lost after removal of the distal half of the tail, the gradient of the attractant is gradually reduced in the tail. The first subchordal cell precursor migrates in the correct direction as the gradient has already formed before amputation, but migration of the second one becomes aberrant because of the delay in the timing of entering the tail.

recording and fluorescent cell labeling demonstrated that these are distinct cell populations. Similarly, the oral gland precursor also has an origin distinct from that of endodermal strand cells. The oral gland precursor and subchordal cell precursors initiate migration from the posterior region of the trunk at almost same stage during larval development. Although their physiological functions are unknown, they have some shared features: they contain many vesicles and mitochondria, and the shape of their nuclei is irregular and variable at the adult stage (Fredriksson and Olsson, 1981, 1991). In the class Appendicularia, species having an oral gland always possess subchordal cells, whereas species lacking an oral gland do not (Galt and Fenaux, 1990). It has been suggested that the oral gland precursor and subchordal cell precursors share some functional or lineage relationship, as they originate from a similar region of the trunk. Therefore, they could share the same embryonic origin.

The endodermal strand cells migrate collectively and are retracted into the trunk in *O. dioica*. Cell tracing analysis using nls-Kaede showed that the endodermal strand cells eventually gave rise to the rectum. In the ascidians *H. roretzi* (Hirano and Nishida, 2000) and *Ciona intestinalis* (Nakazawa et al., 2013), it has been shown that the larval endodermal strand cells give rise to the posterior digestive tract of adults. In *C. intestinalis*, endodermal strand cells migrate to the trunk before tail absorption during metamorphosis (Nakazawa et al., 2013). Thus, the migration of endodermal strand cells is conserved between ascidians and appendicularians. These studies highlight the importance of the larval endodermal strand for formation of the adult digestive organs.

The oral gland precursor and subchordal cell precursors showed lamellipodium-like activity during their migration. In contrast, endodermal strand cells collectively move in a single line without any obvious lamellipodium. Upon removal of the trunk, these precursors exited from the anterior cut edge. In various forms of collective cell migration, front 'leader' cells guide 'followers' at their rear (Friedl and Gilmour, 2009). Our observations and experiments, however, suggest that endodermal strand cells do not require anterior cells for migration. It is not yet clear whether endodermal strand cells themselves have the capacity to migrate, or whether flanking cells, epidermis, muscle and notochord push the endodermal strand cells, although no change in the shape of these flanking cells was evident. The direction of endodermal strand cell movement is already determined by the hatching stage, as revealed by amputation experiments. The directional information might be present in the flanking cells, or gradients of certain molecules might be preformed in the intercellular space.

It is striking that the syncytial oral gland precursor became U-shaped, and then eventually separated into left and right cells, after which the four nuclei showed an invariant pattern of partitioning during separation. To our knowledge, this is the first report of such a directional movement and specific behavior of a syncytium during animal morphogenesis, although some cells migrate as a syncytium or a coenocyte, such as leukocytes and slime mold plasmodia. The mechanisms for achieving this interesting form of cell behavior are unknown, but further analyses are clearly warranted.

Lamellipodia are observed in individual subchordal cell precursors. These precursors did not require any influence from the trunk, while removal of the distal half of the tail affected the direction of their migration. In many cases during animal development, directed cell migration is mediated by chemoattractants or chemorepellents. For example, in the posterior lateral line in fish, Cxcl12a, a chemokine, and FGF work as chemoattractants (David et al., 2002; Lecaudey et al., 2008). It is possible that a gradient of diffusible chemoattractant emanates from the tip of the tail, and that this gradient, if present, would gradually diminish after removal of the distal half of the tail (Fig. 6B). Removal of the distal half of the tail more severely affected the movement of the second subchordal cell. Two of the subchordal cell precursors show different timing for entering the tail. The first one would be able to migrate in the correct direction in the presence of the preexisting gradient. The second one would also utilize the gradient initially, but at a later stage it might lose its direction because of temporal diminution of the gradient (Fig. 6B). It would also be interesting to investigate the mechanisms

responsible for cessation of migration, preventing them from reaching the far tip of the tail (Fig. 2A) and suddenly stopping them from moving at almost the same time while a constant distance is maintained between the two cells.

The migration of the endodermal strand is considered to involve collective migration of a strand of 16 cells. The oral gland precursor migrates as a single syncytium and shows unique movements. The migration of subchordal cell precursors is categorized as individual cell migration. Therefore, these types of cell migration in *O. dioica* provide unique opportunities for comprehensively understanding the versatility of cell migration movements in a simple organism possessing a chordate body plan. Fluorescent cell labeling is a practical technique for characterizing the developmental processes occurring in *O. dioica*. Since mRNA encoding fluorescent markers is injected into the ovary, the fluorescent label can be visualized from the beginning of embryogenesis at the unfertilized egg stage in many eggs by means of a single microinjection (Omotezako et al., 2013). The fluorescence lasts at least until 10 hpf (7 hph), when larvae complete organogenesis and form a functional body. In combination with the rapid development of *O. dioica*, the live imaging employed in the present study will be useful for visualizing every process of embryogenesis and larval organogenesis at single-cell resolution in this model chordate.

Acknowledgments

We thank to Dr. A. Nishino for the instruction and insightful discussion. M. Suzuki provided useful help with the culture of *O. dioica*. This work was supported by Grants-in-Aid for Scientific Research from the JSPS to HN (22370078 and 26650079), and to TAO (24870019).

References

Aman, A., Piotrowski, T., 2010. Cell migration during morphogenesis. Dev. Biol. 341, 20–33.

Ando, R., Hama, H., Yamamoto-Hino, M., Mizuno, H., Miyawaki, A., 2002. An optical marker based on the UV-induced green-to-red photoconversion of a fluorescent protein. Proc. Natl. Acad. Sci. U.S.A. 99, 12651–12656.

Bouquet, J.M., Spriet, E., Troedsson, C., Ottera, H., Chourrout, D., Thompson, E.M., 2009. Culture optimization for the emergent zooplanktonic model organism *Oikopleura dioica*. J. Plankton Res. 31, 359–370.

Conklin, E.G., 1905. The organization and cell lineage of the ascidian egg. J. Acad. Nat. Sci 13, 1–119.

David, N.B., Sapède, D., Saint-Etienne, L., Thisse, C., Thisse, B., Dambly-Chaudière, C., Rosa, F.M., Ghysen, A., 2002. Molecular basis of cell migration in the fish lateral line: role of the chemokine receptor CXCR4 and of its ligand, SDF1. Proc. Natl. Acad. Sci. U.S.A. 99, 16297–16302.

Delsman, H.C., 1910. Beitrage zur Entwicklungsgeschichte von *Oikopleura dioica*. Verh. Rijksinst. Onderz. Zee 3, 1–24.

Delsman, H.C., 1912. Weitere beobachtungen uber die entwicklung von *Oikopleura dioica*. Tijdschr. Ned. Dierk. Ver 12, 199–206.

Fenaux, R., 1998. Anatomy and functional morphology of the appendicularia. In: Bone, Q. (Ed.), The Biology of Pelagic Tunicates. Oxford University Press, pp. 25–34.

Fredriksson, G., Olsson, R., 1981. The oral gland cells of *Oikopleura dioica* (Tunicata Appendicularia). Acta Zool. 62, 195–200.

Fredriksson, G., Olsson, R., 1991. The subchordal cells of *Oikopleura dioica* and *O. albicans* (Appendicularia, Chordata). Acta Zool. 72, 251–256.

Friedl, P., Gilmour, D., 2009. Collective cell migration in morphogenesis, regeneration and cancer. Nat. Rev. Mol. Cell Biol. 10, 445–457.

Fujii, S., Nishio, T., Nishida, H., 2008. Cleavage pattern, gastrulation, and neurulation in the appendicularian, *Oikopleura dioica*. Dev. Genes Evol. 218, 69–79.

Galt, C.P., Fenaux, F., 1990. Urochordata - Larvacea. In: Adiyodi, K.G., Adiyodi, R.G. (Eds.), Reproductive Biology of Invertebrates, Vol. 4, Part B, Wiley-Interscience Publication, pp. 471–500.

Ganot, P., Bouquet, J.M., Kallesøe, T., Thompson, E.M., 2007. The *Oikopleura* coenocyst, a unique chordate germ cell permitting rapid, extensive modulation of oocyte production. Dev. Biol. 302, 591–600.

Ghysen, A., Dambly-Chaudière, C., 2004. Development of the zebrafish lateral line. Curr. Opin. Neurobiol. 14, 67–73.

Hirano, T., Nishida, H., 2000. Developmental fates of larval tissues after metamorphosis in the ascidian, *Halocynthia roretzi*. II. Origin of endodermal tissues of the juvenile. Dev. Genes Evol. 210, 55–63.

Knecht, A.K., Bronner-Fraser, M., 2002. Induction of the neural crest: a multigene process. Nat. Rev. Genet. 3, 453–461F.

Kwan, K.M., Otsuna, H., Kidokoro, H., Carney, K.R., Saijoh., Y., Chien., C.B., 2012. A complex choreography of cell movements shapes the vertebrate eye. Development 139, 359–372.

Lecaudey, V., Cakan-Akdogan, G., Norton, W.H., Gilmour, D., 2008. Dynamic Fgf signaling couples morphogenesis and migration in the zebrafish lateral line primordium. Development 135, 2695–2705.

Nakazawa, K., Yamazawa, T., Moriyama, Y., Ogura, Y., Kawai, N., Sasakura, Y., Saiga, H., 2013. Formation of the digestive tract in *Ciona intestinalis* includes two distinct morphogenic processes between its anterior and posterior parts. Dev. Dyn. 242, 1172–1183.

Nishida, H., 1987. Cell lineage analysis in ascidian embryos by intracellular injection of a tracer enzyme. Dev. Biol. 121, 526–541.

Nishida, H., 2008. Development of the appendicularian *Oikopleura dioica*: culture, genome, and cell lineages. Dev. Growth Differ. 50, S239–S256.

Omotezako, T., Nishino, A., Onuma, T.A., Nishida, H., 2013. RNA interference in the appendicularian *Oikopleura dioica* reveals the function of the *Brachyury* gene. Dev. Genes Evol. 223, 261–267.

Raz, E., 2004. Guidance of primordial germ cell migration. Curr. Opin. Cell Biol. 16, 169–173.

Richardson, B.E., Lehmann, R., 2010. Mechanisms guiding primordial germ cell migration: strategies from different organisms. Nat. Rev. Mol. Cell Biol. 11, 37–49.

Stach, T., Winter, J., Bouquet, J.M., Chourrout, D., Schnabel, R., 2008. Embryology of a planktonic tunicate reveals traces of sessility. Proc. Natl. Acad. Sci. U.S.A. 105, 7229–7234.

Troedsson, C., Ganot, P., Bouquet, J.M., Aksnes, D.L., Thompson, E.M., 2007. Endostyle cell recruitment as a frame of reference for development and growth in the urochordate *Oikopleura dioica*. Biol. Bull. 213, 325–334.